MR Evaluation of Multiple Myeloma at 3.0 Tesla: How do bone marrow signal intensity and selection of protocols affect lesion conspicuity?

Miyuki Takasu[1], Yoko Kaichi[1], Miho Ishikawa[1], Yuji Akiyama[1], Shuji Date[1], Akira Sakai[2], Yoshiaki Kuroda[3], and Kazuo Awai[1]

[1]*Department of Diagnostic Radiology, Graduate School of Biomedical Sciences, Hiroshima University, Hiroshima, Japan,* [2]*Department of Radiation Life Sciences, Fukushima Medical University School of Medicine, Fukushima, Japan,* [3]*Department of Hematology, Hiroshima University Hospital, Hiroshima, Japan*

Target audience: Diagnostic radiologists.

Introduction: The Durie-Salmon PLUS staging system for multiple myeloma takes into account the number of lesions detected by MRI because the number of lesions correlates with overall survival[1]. However, counting focal lesions can be somewhat confusing, because variegated or diffuse patterns of tumor cell infiltration are present in 57% of TI-weighted images[2], which can confound detection of focal lesions. The optimal MRI sequence for detection of focal bone lesions thus remains to be determined. The iterative decomposition of water and fat with echo asymmetry and least-squares estimation (IDEAL) can be used to separate fat and water with very high SNR efficiency, thereby resulting in robust fat suppression[3]. The present study compared T1-weighted, fat-suppressed T2-weighted FSE (FS-T2 FSE), STIR, and T2-weighted FSE IDEAL sequences in terms of CNR and percent contrast and assessed the dependence of lesion conspicuity on background bone marrow (BM) signal intensity in multiple myeloma.

Methods: Spinal MRI was performed in 54 patients with multiple myeloma. Imaging was performed using a 3.0-T MRI unit (Signa HDxt 3T; GE Healthcare) with sagittal T1 fast spin-echo-weighted imaging (T1 FSE); FS-T2 FSE (with the CHESS technique); fast STIR imaging; and IDEAL T2 fast spin-echo-weighted sequence (TR/TE, 4000/112.4 ms; averages, 6; matrix size, 448×288; FOV, 300 mm; slice thickness, 4 mm; band width, 83.3 kHz; ETL, 16; acquisition time, 6 min 17 s). Co-registered water and fat images were generated by the IDEAL software. Mean signal intensity and standard deviation were calculated by placing operator-determined regions of interest (ROI) within the focal myeloma lesions (FL), in the BM of the L1-L3 vertebral bodies and the spinal cord (SC). BM Signal intensity was calculated as the mean value obtained from the three vertebral bodies. For each MRI examination, CNR and the percent contrast between BM and SC (n=54) and between BM and FL (n=20) were measured using the following equations:

$$\text{Percent contrast} = (S_a - S_b)/(S_a + S_b)$$

$$\text{CNR} = |S_a - S_b|/((S_{asd}^2 + S_{bsd}^2)/2)^{1/2}$$

where S_a and S_b are mean intensity and S_{asd} and S_{bsd} are the standard deviation of intensities for the investigated lesion or normal tissues. Fat-signal fraction from IDEAL images was calculated from the ratio of the signal intensity in the fat image divided by the signal intensity of the corresponding ROI in the in-phase image. Spearman rank correlation coefficients (ρ) were calculated to investigate possible correlations between percent contrast and the fat signal fraction. One-way analysis of variance with Scheffé's post hoc test was used to compare CNR and percent contrast among the four different groups (i.e., T1 FSE, FS-T2 FSE, fast STIR, and water image of IDEAL) for all patients.

Table 1. Results of Spearman rank correlation for percent contrast with fat signal fraction.

Sequence	ρ	*p*
Water image of IDEAL	0.753	<0.0001
Fat-suppressed T2 FSE	0.850	<0.0001
Fast STIR	0.572	<0.0001
T1 FSE	-0.160	0.25

Results: Table 1 and Figure 1 show a significant correlation between percent contrast and fat signal fraction, except for in the T1-FSE. Therefore, we categorized patients into one of two groups: a T1-dark marrow group (n=15), with fat signal fraction <50%; and a T1-bright marrow group (n=39), with fat signal fraction ≥ 50%. BM-SC CNR was significantly greater for the water image of IDEAL and FS-T2 FSE than for the STIR. BM-FL CNR was significantly higher for the FS-T2 FSE than for the STIR in T1-bright marrow (p<0.05), but no significant difference was found in the T1-dark marrow among the three fat-suppression methods. Figure 2 shows that the BM - SC percent contrast was significantly higher for FS-T2 FSE than for the STIR. In T1-bright marrow, percent contrast was significantly higher for FS-T2 FSE than for the water image of IDEAL ($p < 0.05$). BM-FL percent contrast in T1-bright marrow was significantly greater for the FS-T2 FSE than for the STIR ($p < 0.05$), but no significant difference in T1-dark marrow was found among three fat-suppression methods.

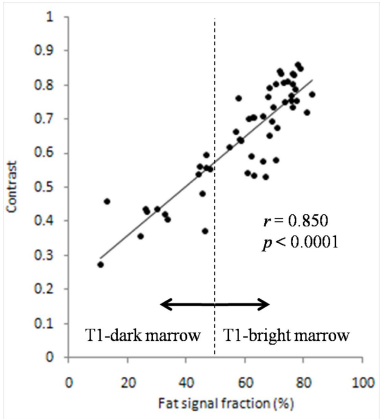

Figure 1. Graph of the fat signal fraction versus percent contrast for FS-T2 FSE. Linear regression curve was plotted. Vertical line corresponds to a fat signal fraction of 50%.

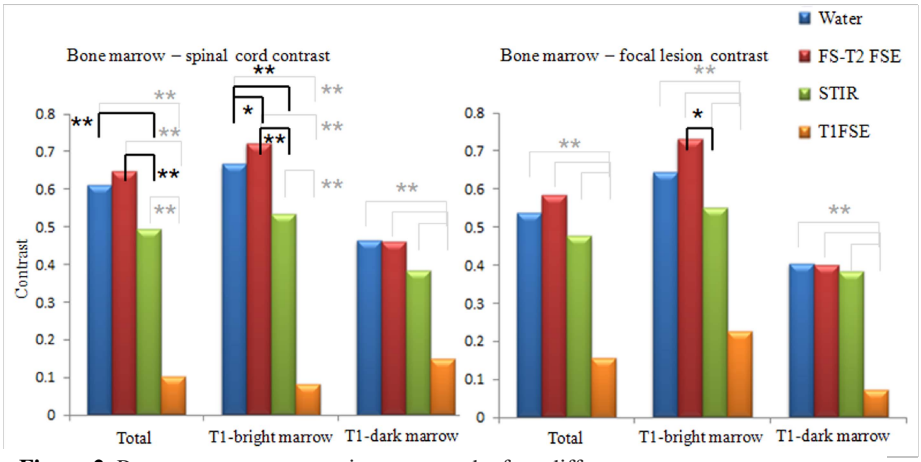

Figure 2. Percent contrast comparison among the four different sequences.

Discussion: The STIR in this study showed significantly lower CNR and percent contrast when compared with the FS-T2 FSE. This finding can be explained by the improvement of the saturation pulse of the CHESS technique in 3-T MRI. In this study, BM-FL CNR and percent contrast in T1-dark marrow were significantly lower when compared with those in T1-bright marrow. This result means that detection of focal myeloma lesions is more difficult in T1-dark marrow than in T1-bright marrow. In patients with multiple myeloma, four different infiltration patterns can be seen on MRI: normal-looking bone marrow corresponding to slight interstitial plasma cell infiltration; focal myeloma infiltration; diffuse bone marrow infiltration, characterized by a homogeneous decrease in signal on T1-weighted SE images and increased signal intensity on fat-suppressed images; and a combined focal and diffuse infiltration pattern. We attributed the lower CNR and percent contrast on fat-suppressed images of the T1-dark marrow to increased signal intensity of bone marrow mainly caused by T2 prolongation due to diffusely infiltrated myeloma cells.

Conclusion: Conspicuity of focal myeloma lesion in the spinal bone marrow was dependent on the fat signal fraction in fat-suppressed MRI. The FS-T2 FSE showed higher percent contrast than all other sequences. No significant difference in lesion conspicuity was found among fat suppression techniques in T1-dark marrow, suggesting the need for an inclusive, multimodality imaging approach including CT or PET to evaluate focal lesions in multiple myeloma.

References: 1. Walker R, et al. Magnetic resonance imaging in multiple myeloma. J Clin Oncol 2007;25:1121-1128. 2. Baur-Melnyk A, et al. Role of MRI for the diagnosis and prognosis of multiple myeloma. Eur J Radiology 2005;55:56–63. 3. Reeder SB, Wen Z, Yu H et al. Multicoil Dixon chemical species separation with an iterative least-squares estimation method. Magn Reson Med 2004;51:35–45.